scientific reports

Check for updates

OPEN

Impact of removal frequency on site-specific force profile and dimensional stability of clear aligners in relation to dental crowding

Jin-Young Choi[1,4], Nurdana Darkhanbayeva[1,4], Min-Ji Jeon[1], Kun-Woo Park[1], Hoon Kim[2], Jung-Yul Cha[3] & Su-Jung Kim[1]✉

This in vitro comparative study examined the effects of high removal frequency on force generation and gap width changes in direct-printed aligners (DPAs) compared with thermoformed aligners (TFAs), considering different tooth positions and crowding conditions. A total of 104 aligners, comprising 26 pairs of DPAs and 26 pairs of TFAs, were fabricated for both crowded and noncrowded maxillary arch models. Force measurements were conducted at initial placement and after every 20 removal cycles for up to 100 cycles, whereas gap width analyses were performed at initial placement and after 100 removal cycles. Statistical analyses were performed to evaluate the force and gap width changes, with a focus on site-specific differences. DPAs demonstrated significantly lower initial forces and maintained consistent force levels over increased removal frequencies, irrespective of crowding conditions. Conversely, TFAs exhibited higher initial forces, with significant force decay over time, particularly in crowded models. DPAs also showed improved fit over time with decreased gap widths, whereas the gap widths of TFAs increased, particularly in the gingival areas. DPAs offer superior dimensional stability and force predictability over TFAs while maintaining consistent performance across different tooth positions and crowding scenarios.

Keywords Direct-printed aligner, Thermoformed aligner, Force decay, Dimensional stability, Dental crowding

The introduction of clear aligners (CAs) has contributed to notable changes in orthodontic treatment by providing an aesthetic, comfortable, hygienic, and convenient alternative to fixed appliances[1], which are often preferred by patients[2–4]. Moreover, advances in materials and manufacturing methods have significantly enhanced the clinical performance of CAs, thereby expanding their applicability to various types of malocclusions[5–7]. The integration of digital technology with three-dimensional (3D) printing has minimized labor-intensive fabrication and reduced cumulative processing errors associated with traditional thermoplastic workflows[8]. Direct-printed aligners (DPAs), which bypass the intermediary step of 3D model printing, utilize innovative materials[9], such as photopolymerizable polyurethane (Tera Harz TC-85 DAC UV Resin; Graphy Inc., Seoul, Korea). This advancement enables same-day appliance delivery via in-house fabrication. Although DPAs are known for their shape memory properties and dimensional stability at high temperatures, recent studies have reported that in-house 3D-printed aligners may exhibit a higher relaxation index and a more rapid force decline compared to conventional thermoformed aligners (TFAs)[10]. Nevertheless, their unique material properties could still offer advantages in force predictability, which warrants further investigation and nuanced discussion.

To achieve planned tooth movements, CAs must exert controlled forces on target teeth with minimal unintended force fluctuation decay. Understanding the mechanical properties of a material that affects the biomechanical behavior of the appliance is crucial. However, evidence is limited because of the complexity of analyzing the entire arch force system exerted by CAs. Studies have explored various mechanical properties

[1]Department of Orthodontics, Kyung Hee University College of Dentistry, Kyung Hee University Dental Hospital, Seoul, Republic of Korea. [2]Graphy Inc, Seoul, Republic of Korea. [3]Department of Orthodontics, Institute of Craniofacial Deformity, Yonsei University College of Dentistry, Seoul, Republic of Korea. [4]Jin-Young Choi and Nurdana Darkhanbayeva equally contributed to this work. ✉email: ksj113@khu.ac.kr

of DPAs, including their thermomechanical characteristics, viscoelasticity, stress relaxation and creep, shape recovery, ultraviolet (UV) curing kinetics, and cytotoxicity[11–18]. Ensuring the dimensional accuracy of DPAs is critical for optimal fit and stability throughout the treatment period. Any discrepancy in fit may lead to insufficient physiological activation of alveolar remodeling or excessive force on the teeth, complicating the force system and making it unpredictable. Therefore, maintaining close contact between the aligner and tooth surfaces is essential despite repeated mechanical stresses over time[19]. Notably, manufacturers recommend a minimum gap width of 50 µm for fabrication purposes, as supported by recent micro-CT studies[20]. This raises questions regarding whether DPAs fit the reference model better than TFAs prior to activation in the mouth.

Previous studies compared the dimensional accuracies of DPAs and TFAs under various conditions and yielded mixed results. Studies using metrology software for alignment have shown that DPAs fit more accurately than TFAs, suggesting that DPAs deliver more aligned forces with biologically desired levels and biomechanically consistent profiles[13,21]. Conversely, based on site-specific morphometric analyses, a recent micro-computed tomography (CT) study found greater gap widths in DPAs than in TFAs, particularly in the palatal, buccogingival, and palatogingival regions, based on site-specific morphometric analyses[20]. Moreover, dimensional stability after repeated aligner deflection due to frequent insertion and removal is vital for consistent force delivery. Although studies have shown decreased forces in TFAs with increased removal frequency[22], similar investigations on DPAs are lacking. An in vivo study on DPAs[10] indicated no significant changes in the mechanical properties after 1 week of intraoral aging, although the sample size was limited.

Predicting the force levels delivered to each tooth remains challenging because tooth movement with CAs is not solely dependent on the shape-molding effect. Various factors influencing the loading force changes have been identified, including material properties, degradation over time, removal frequency, tooth irregularity, and inbuilt activation[22]. However, it is crucial to minimize the discrepancies between the intimate contact areas and relief areas within activated aligners[23]. Before assessing the viscoelastic properties, it is important to verify the effect of the aligner removal frequency on non-activated aligners by correlating force changes with gap width alterations due to deformation.

This in vitro study aimed to investigate the site-specific effects of removal frequency on the dimensional stability and consequent loading force changes in DPAs compared with TFAs, focusing on the central incisor, canine, second premolar, and second molar regions within a crowded dental arch. The null hypothesis posited that DPAs would exhibit no significant changes in gap width and force levels across all tooth surfaces after repeated appliance removal, regardless of tooth position or anterior crowding.

Methods

Sample preparation

A master scan of the maxillary arch with well-aligned occlusion after orthodontic treatment was obtained using an intraoral scanner (Trios, 3shape, Copenhagen, Denmark) for control purposes. The standard tessellation language (STL) file was imported into the 3D setup software (DentOne, Diorco Co., Ltd., Seoul, Korea; https://www.ezdentone.com/) to create another STL file of the maxillary arch with a tooth-size-arch-length discrepancy of 6 mm for the study sample. Two types of digital master models were produced: one with crowding and one without crowding. Ten master models were printed for each group using a digital light processing (DLP) 3D printer (Asiga UV MAX385, Asiga, Alexandria, Australia) at a 50-µm layer thickness. A total of 104 aligners were fabricated: 26 pairs of DPAs (DPA_C and DPA_NC) and 26 pairs of TFAs (TFA_C and TFA_NC) for both the crowding (C) and non-crowding (NC) groups (Fig. 1). In each aligner group, 20 pairs were used for the film-sensor tests and 6 pairs were used for micro-CT analysis. The sample size per subgroup (tooth position/crowding condition) was estimated to be at least 16, as determined using the G* Power software (version 3.1.9.7, Düsseldorf, Germany), according to previous studies[22]. An effect size of 0.4, a power of 90%, and an α value of 0.05 were applied.

DPA fabrication

DPAs were digitally designed using aligner design software (Deltaface, Coruo, Limoges, France; https://deltaface.com/) with a predetermined thickness of 0.50 mm and an offset of 50 µm. The aligner margins on the facial sides were digitally trimmed to approximately 1 mm below the gingival margins, following the natural contour. They were positioned at a printing angle of 30° for minimal support struts and printed using a TC-85DAC 3D Printing Shape Memory Aligner Resin (Graphy Inc., Seoul, Korea) and a DLP 3D printer (Asiga UV MAX385, Asiga, Alexandria, Australia). The residual resin was removed from the printed aligners by using a centrifuge (Tera Harz Spinner, Graphy Inc., Seoul, Korea) at 500 rpm for 5 min. The DPAs were then cured for 20 min with UV light (405 nm) under nitrogen atmosphere using a post-curing machine (Tera Harz Cure, Graphy Inc., Seoul, Korea). The final cleaning was performed using an ultrasonic cleaner for 2 min at 80 °C.

TFA fabrication

A 0.75-mm thickness of polyethylene terephthalate glycol (PET-G) sheet, branded as Easy-Vac Gasket (3A MEDES, Korea), was utilized to vacuum-thermoform the passive aligner over the printed master models using a pressurized thermoforming machine (Biostar, Scheu-Dental, Iserlohn, Germany), following the manufacturer's recommendations. The thermoformed sheet was removed from the model and trimmed along the same gingival edges as the DPA. All TFAs ($n = 52$) were produced by a single technical expert (ND) using the same master model of the TFA_C or TFA_NC samples.

Force measurement

A thin-film single pressure sensor (FlexiForce ESS102, Tekscan Inc. USA) was used, which operates on a piezoresistive principle, where applied force changes the electrical resistance of the sensing element, enabling

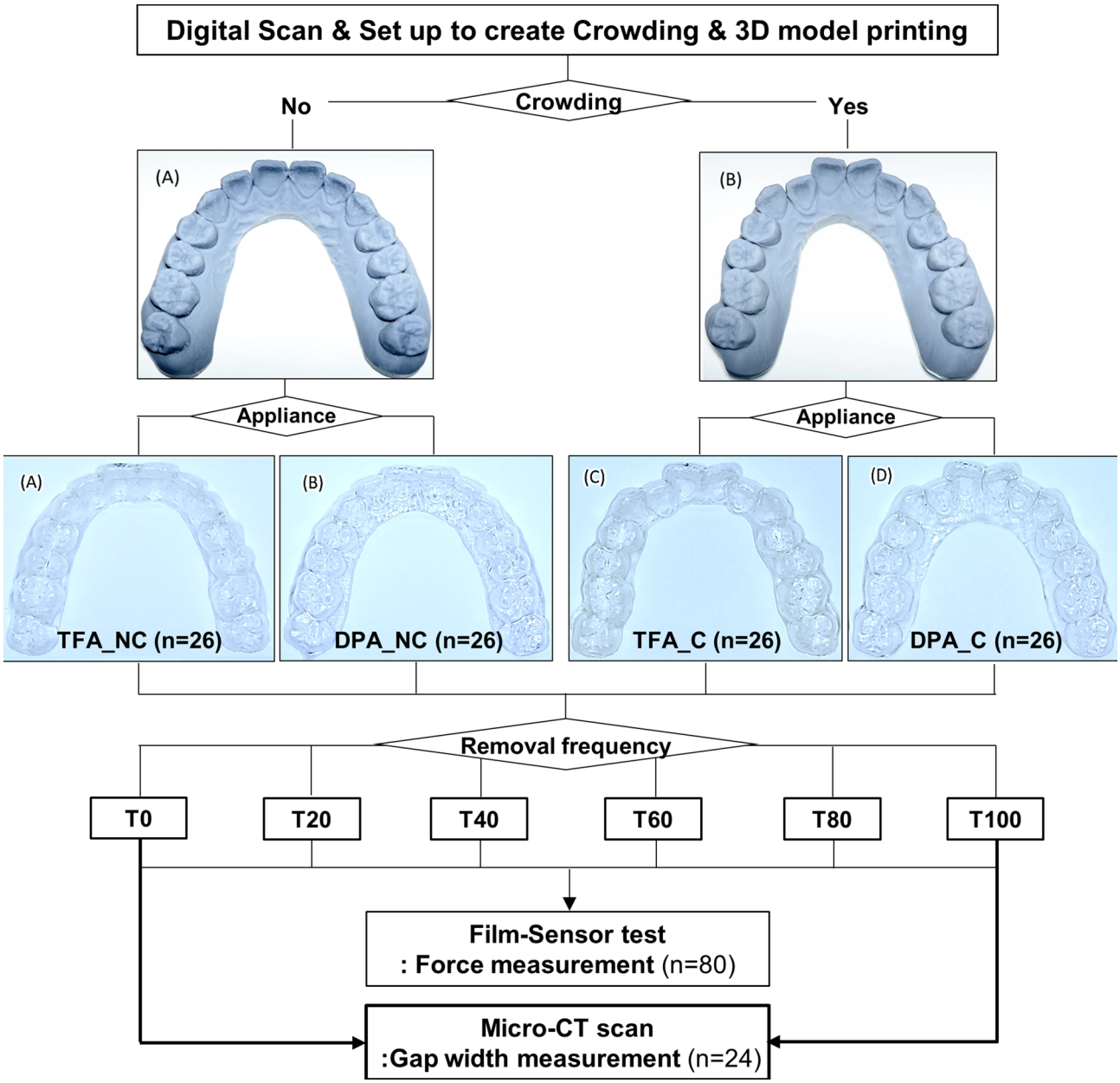

Fig. 1. Diagrammatic flowchart of experimental design. TFA_NC, thermoformed aligner fabricated from a non-crowding model; DPA_NC, direct-printed aligner from a non-crowding model; TFA_C, thermoformed aligner from a crowding model; DPA_C, direct-printed aligner from a crowding model.

force quantification. It measured the compression exerted by the aligners on each tooth surface (Fig. 2A). The sensors, featuring soft and flexible structures with minimal thickness (0.203 mm), a small sensing area (3.8-mm diameter), high sensitivity, and a measurable force range of 4.4 N (448.668 g), were employed. To enhance the accuracy of force measurement and minimize artificial force artifacts caused by the sensor thickness, the master models were digitally modified prior to printing by precisely removing tooth surface areas corresponding to the sensor thickness. This created dedicated spaces that allowed the thin-film pressure sensors to seat flush within the model surface. This ensured intimate contact between the sensor and tooth surface, reducing any gap or misalignment that could lead to measurement errors. To minimize the sensor weight imbalance due to the discrepancy between the flat sensor and curved inner aligner surface, the sensors were trimmed, and tooth surfaces were optimally prepared to enhance sensor performance (Fig. 2B). Four sensors were fixed to the prefabricated facial surfaces of the central incisor, canine, second premolar, and second molar of each master model using cyanoacrylate (Fig. 2C). All sensors were reset and calibrated across different model-sensor-aligner complexes before measurement to ensure consistent loading geometry and environmental conditions. Ten samples were randomly selected for reproducibility testing by precision rate[22], and the averaged precision rate between repeated measurements was found to be 93.2 ± 2.8%.

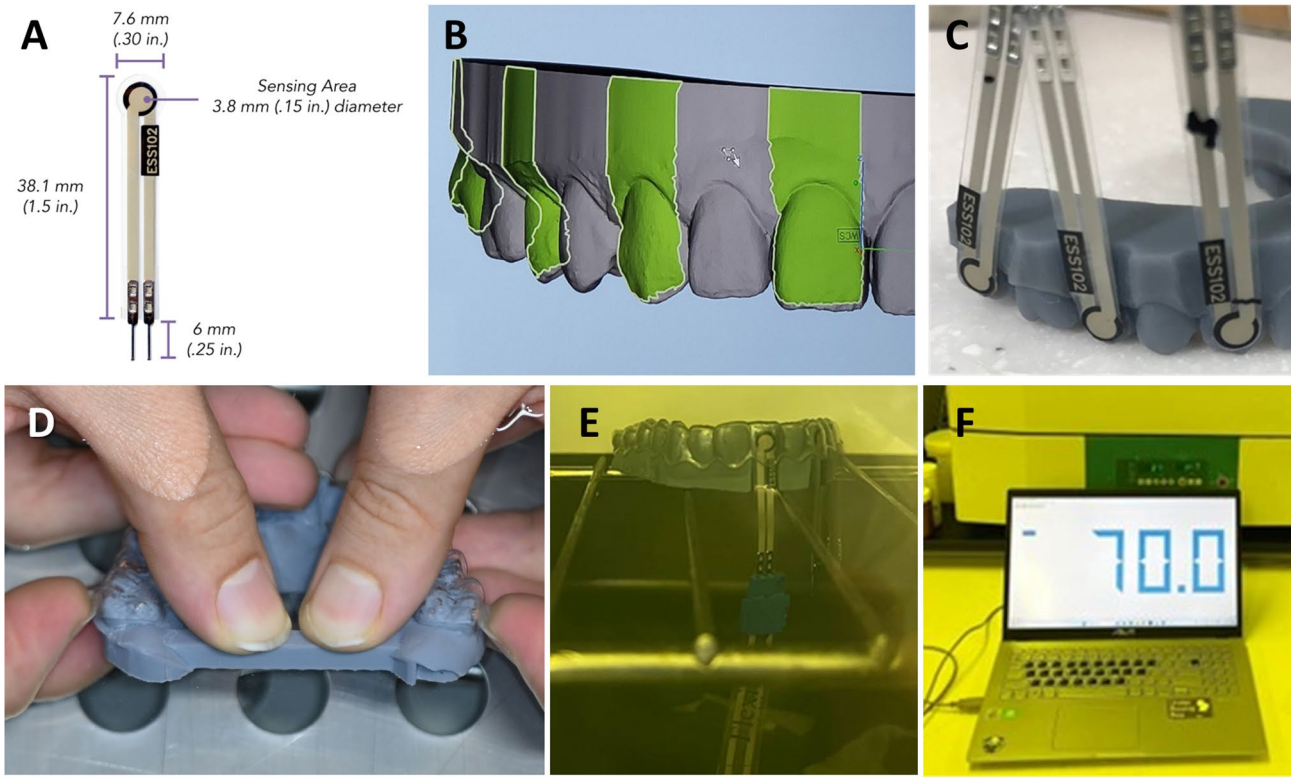

Fig. 2. Force measurement process. (**A**) FlexiForce ESS102 sensors used for measuring forces. (**B**) Digital surface design of the printed model, providing space for sensor placement to ensure the best passive fit of the aligner. (**C**) Sensors attached to the tested teeth surfaces of the printed model. (**D**) Repeated aligner insertion and removal procedure conducted on the master model in a water bath at 40℃. (**E**,**F**) Data collection of force measurements with aligner seated on the prepared model within an oven set at 37℃.

Force measurements were conducted at the initial placement of the aligner (T0), after every 20 removals (T20, T40, T60, and T80), and after removal up to 100 times (T100). The process of placing and removing aligners was performed exactly as orthodontists recommend to patients, according to the aligner type. Typically, patients are instructed to immerse the DPA in warm water at around 45℃ before placement, press the aligner on the occlusal and buccal surfaces to ensure proper seating, and when removing, to hold warm water in their mouth for gentle removal. For TFAs, patients are generally advised to place the aligner at room temperature and remove it by applying alternating forces starting from one posterior tooth on one side and then the other side to prevent deformation. Reflecting these clinical instructions, repeated insertion and removal of DPAs were conducted inside a water bath at 45℃, and force was measured in a laboratory oven set at 37℃ after a one-hour stay to fully express its shape memory property (Fig. 2D). For TFAs, all procedures were performed inside a water bath at 37℃. The entire process was performed by a single technician (ND).

The sensors were calibrated using a static weight calibration procedure to ensure accurate force measurement. 5, 10, and 20 g weights were gently applied onto each sensor placed on the prepared flat surface. Each calibration weight was placed to fully cover the sensor's active area, ensuring even load distribution. Each sensor was calibrated individually, and the calibration files were saved. Calibration curves from individual sensors were compared to verify measurement consistency across sensors. Linear interpolation between calibration points was used to convert sensor output values to actual force during experiments. Prior to calibration, each sensor was conditioned by repeatedly applying approximately 110% of the maximum test load to stabilize sensor response and minimize drift and hysteresis. Calibration was performed at room temperature, matching the measurement conditions. The sensor wiring was connected to the data acquisition system and managed with the ELF system software (Tekscan Inc., USA), and the signals were digitized at a sampling rate of 200 Hz. All force data were automatically collected and logged during each measurement session. Figure 2E,F illustrate the measurement setup, including sensor connection and aligner seating on the model within the temperature-controlled chamber.

Gap width measurement

All aligners over the corresponding master models in the TFA_C, TFA_NC, DPA_C, and DPA_NC groups ($n = 6$ each) were scanned at T0 and T100 using a high-resolution micro-CT (Skyscan1173, Bruker, MA, USA) at 40 kV, 200 µA, and 35-µm resolution. The resulting 3D images ($n = 48$) of each target tooth were reoriented using the DataViewer software (version 1.5.6.2, Bruker, Kontich, Belgium; https://www.bruker.com/en/products-and-solutions/preclinical-imaging/micro-ct/3d-suite-software.html). Midsagittal longitudinal slices perpendicular to both the model base plane and the line linking the most mesial and distal contact points were obtained for

the central incisors and canines (Fig. 3A). Longitudinal slices were constructed for the premolars and molars that passed through the facial and palatal cusp points (FC and PC, respectively) (Fig. 3B). An example of the longitudinal slice obtained for the second molar using this procedure is presented in Fig. 3C. Gap widths were measured using the CTAn software (release 2.5, Bruker, Kontich, Belgium; https://www.bruker.com/en/products-and-solutions/preclinical-imaging/micro-ct/3d-suite-software.html) at 300x magnification as the shortest distance when a perpendicular line was projected from each reference point tangent on the tooth. The reference points included gingival margins, facial and palatal contour heights, incisal edge/cusp points, and the most concave cingulum/occlusal pit: facial (F); faciogingival (FG); palatal (P); palatogingival (PG); and additionally, incisal (IN) for anterior teeth (Fig. 3D); FC, PC, and occlusal fossa (OF) for posterior teeth (Fig. 3E).

Statistical analysis

We performed inter-group comparisons of forces at different aligner removal frequencies between DPAs and TFAs according to tooth position and presence of crowding. In addition, the gap width differences between the model and aligner after 100 removal cycles and the DPAs and TFAs across various tooth regions in both the C and NC groups were compared.

This was confirmed using a linear mixed-effects model for repeated data, and the interaction effects between the removal point, appliance, and crowding were evaluated through the interaction term. Additionally, multiple comparisons using Bonferroni post-hoc correction were carried out.

All statistical analyses were performed based on a significance level of 0.05, and SAS9.4 (SAS Institute, Inc., Cary, NC) and R4.4.2 (https://cran.r-project.org) were used for statistical analyses. Author JC and ND conducted the data analysis with consultation from expert statisticians to ensure rigorous statistical evaluation.

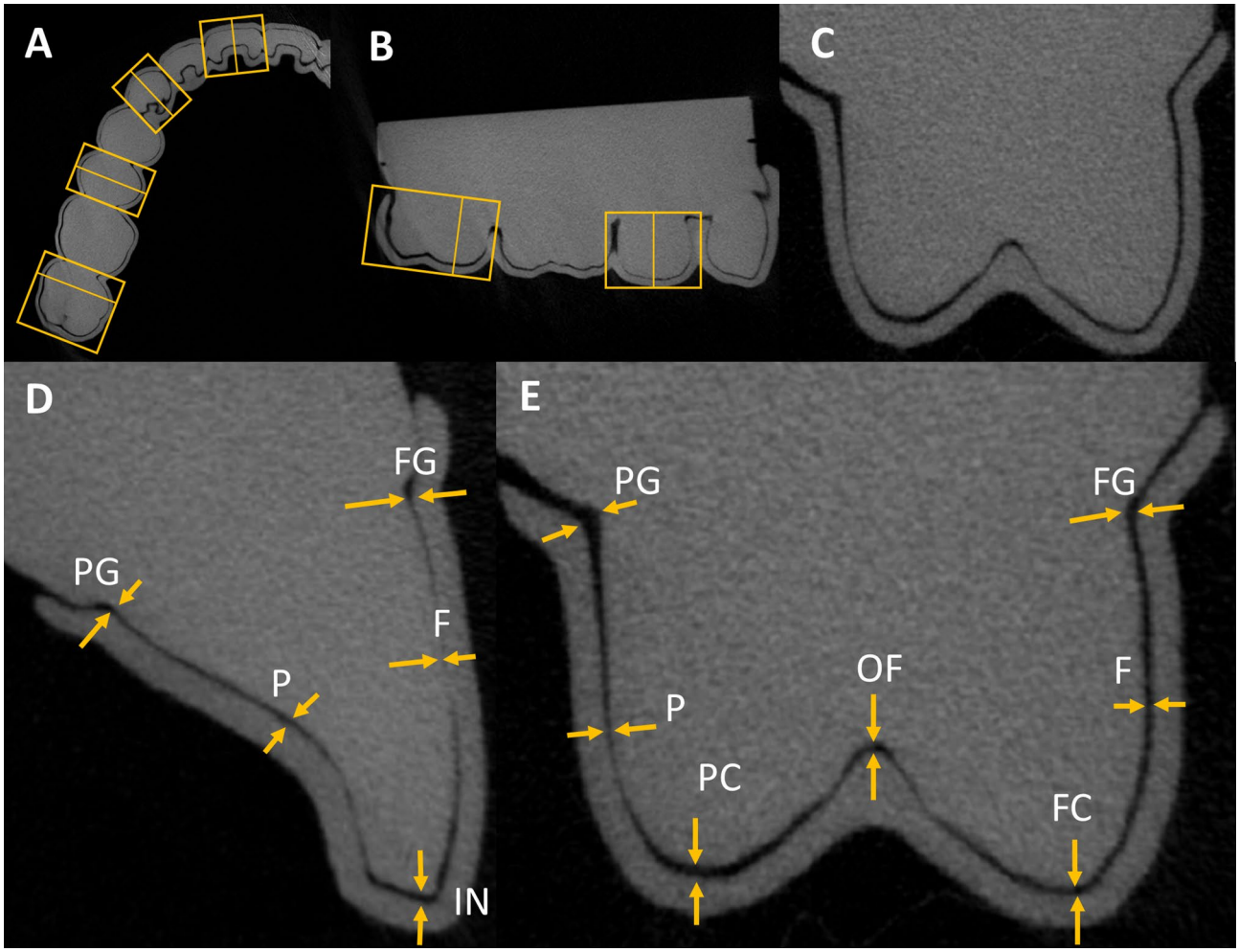

Fig. 3. Micro-CTs illustrating the gap width between aligners and teeth at reference points. (**A**) Axial view showing the region settings for each tooth. (**B**) Sagittal view showing the region settings for each tooth. (**C**) Micro-CT cross-sectional images of the designated region. (**D**) Anterior teeth (e.g., the central incisor). (**E**) Posterior teeth (e.g., the second premolar). Yellow arrows indicate the reference points on the teeth.

Results

Comparison of the force levels between aligners at different removal frequencies

At the initial placement (T0), DPA exerted significantly lower forces than TFA did in the C and NC groups across all tested teeth (Table 1). The forces delivered by TFA were notably lower in the C group (20.81 ± 10.94 g to 79.15 ± 18.35 g) compared with the NC group (132.75 ± 46.19 g to 181.64 ± 46.36 g) at all tested frequencies up to T100, except for the second molars. In contrast, the forces exerted by DPA showed no differences between the groups based on crowding or tooth position and remained within a narrow range (4.68 ± 1.23 g to 7.58 ± 0.70 g).

Comparison of force changes between aligners: effects of crowding and tooth position

The linear mixed-effects model for repeated measures indicated that the forces exerted by TFA significantly decreased with increasing removal frequency in the NC and C groups. However, the forces exerted by DPA showed no significant changes over time in either group (NC or C). Regarding the relative force rate at each removal frequency, the greatest reduction was observed in the TFA_C group, followed by the TFA_NC group, whereas the DPA_C and DPA_NC groups maintained consistent force levels across all removal frequencies. This trend was most pronounced in the central incisors, where the relative force levels were 61.05%, 81.69%, 101.53%, and 100.64% in the TFA_C, TFA_NC, DPA_NC, and DPA_C groups, respectively. A linear mixed-effects model with interaction terms revealed significant effects of crowding on the force levels for the central incisors, canines, and second premolars in the TFA samples only. Specifically, for the central incisor, canine, and

Tooth #	Removal frequency	DPA group		TFA group		P-value of Interaction
		DPA_NC	*DPA_C*	*TFA_NC*	*TFA_C*	
#11	T0	7.47 ± 0.63	6.07 ± 0.75	181.03 ± 43.51	33.20 ± 10.67	
	T20	7.56 ± 0.78	6.13 ± 0.79	169.93 ± 41.60	29.76 ± 10.71	0.328
	T40	7.32 ± 0.73	6.16 ± 0.79	166.60 ± 41.78	29.17 ± 10.97	0.09
	T60	7.55 ± 0.78	6.20 ± 0.67	161.35 ± 38.40	24.85 ± 10.62	< 0.001***
	T80	7.48 ± 0.55	6.17 ± 0.63	156.03 ± 37.72	23.41 ± 10.43	< 0.001***
	T100	7.58 ± 0.70	6.11 ± 0.81	148.51 ± 39.41	20.81 ± 10.94	< 0.001***
	P-value†	0.285	0.378	<0.001†††	<0.001†††	< 0.001***
	P-value‡	0.916		<0.001‡‡‡		
#13	T0	4.74 ± 1.23	5.34 ± 0.98	173.74 ± 44.53	79.15 ± 18.35	
	T20	4.71 ± 1.28	5.37 ± 0.84	159.34 ± 42.92	68.82 ± 19.28	0.162
	T40	4.83 ± 1.33	5.36 ± 0.96	154.70 ± 44.24	65.08 ± 18.50	0.261
	T60	4.68 ± 1.23	5.60 ± 1.12	150.06 ± 42.54	61.70 ± 16.75	0.008**
	T80	4.70 ± 1.15	5.43 ± 0.83	145.67 ± 40.67	56.16 ± 16.50	0.003**
	T100	4.83 ± 1.20	5.41 ± 0.80	137.63 ± 40.91	53.15 ± 15.61	0.032*
	P-value†	0.247	0.073	<0.001†††	<0.001†††	0.005**
	P-value‡	0.865		<0.001‡‡‡		
#15	T0	5.95 ± 0.80	6.06 ± 0.66	181.64 ± 46.36	56.50 ± 15.67	
	T20	6.20 ± 0.97	6.20 ± 0.66	164.69 ± 42.62	48.36 ± 16.20	0.586
	T40	6.02 ± 0.87	6.21 ± 0.54	152.76 ± 42.07	46.84 ± 14.72	0.646
	T60	5.87 ± 0.86	6.24 ± 0.52	147.40 ± 44.85	41.69 ± 13.54	0.057
	T80	5.79 ± 0.95	6.10 ± 0.58	143.68 ± 42.84	38.70 ± 11.66	0.02*
	T100	5.94 ± 0.86	6.01 ± 0.68	132.75 ± 46.19	34.99 ± 9.09	0.135
	P-value†	0.098	0.319	<0.001†††	<0.001†††	0.017*
	P-value‡	0.373		0.015‡		
#17	T0	5.07 ± 0.35	5.04 ± 0.44	162.66 ± 44.27	167.07 ± 42.23	
	T20	5.17 ± 0.55	5.16 ± 0.41	144.56 ± 44.97	152.85 ± 36.24	0.573
	T40	5.08 ± 0.48	5.17 ± 0.34	136.76 ± 42.73	145.29 ± 37.16	0.855
	T60	5.20 ± 0.53	5.15 ± 0.36	126.49 ± 39.43	136.95 ± 39.04	0.423
	T80	5.08 ± 0.41	5.22 ± 0.46	117.65 ± 38.24	128.85 ± 36.53	0.76
	T100	5.18 ± 0.38	5.10 ± 0.31	104.12 ± 37.89	118.92 ± 35.77	0.107
	P-value†	0.423	0.221	<0.001†††	<0.001†††	0.177
	P-value‡	0.934		0.085		

Table 1. Inter-group comparisons of forces (g) at different aligner removal frequencies between DPA and TFA, categorized by tooth position and the presence of crowding (values in parentheses represent the relative ratio when T0 is considered as 100). †Analysed by liner mixed-effects model for repeated measures. †, $P < 0.05$; ††, $P < 0.01$; †††, $P < 0.001$. ‡Analysed linear mixed-effects model with interaction terms for removal frequency and appliance. ‡, $P < 0.05$; ‡‡, $P < 0.01$; ‡‡‡, $P < 0.001$. *Analysed linear mixed-effects model with interaction terms for removal frequency, appliance, and crowding presence. *, $P < 0.05$; **$P < 0.01$; ***$P < 0.001$.

second premolar, no significant differences in force were found between the DPA_C and DPA_NC groups at any removal frequency. In contrast, the forces measured in the TFA_NC group were consistently greater than those in the TFA_C group across all time points for these teeth. For the second molar, there was no significant difference in force between the DPA_C and DPA_NC groups, nor between the TFA_NC and TFA_C groups, at any removal frequency (Table 1; Fig. 4). The detailed intra-group and inter-group comparisons of force changes across removal frequencies are presented in Supplemental Table.

Comparison of gap widths between aligners at different tooth surface areas

The initial gap widths (T0) exhibited site-specific differences across all tooth surfaces between DPA and TFA depending on the tooth position (Table 2). In both NC and C groups, TFA exhibited the greatest gap at the PG and OF areas for anterior (173.57 ± 32.36 μm to 298.03 ± 41.74 μm) and posterior teeth (140.71 ± 16.97 μm to 316.26 ± 58.83 μm), respectively, and the smallest gaps at the F surfaces for the anterior teeth (4.06 ± 6.23 μm to 36.79 ± 24.02 μm), indicating a large variation in gap width depending on the location. In contrast, DPA displayed the largest gaps at the IN area for anterior teeth (85.95 ± 19.61 μm to 117.10 ± 26.72 μm) and at the

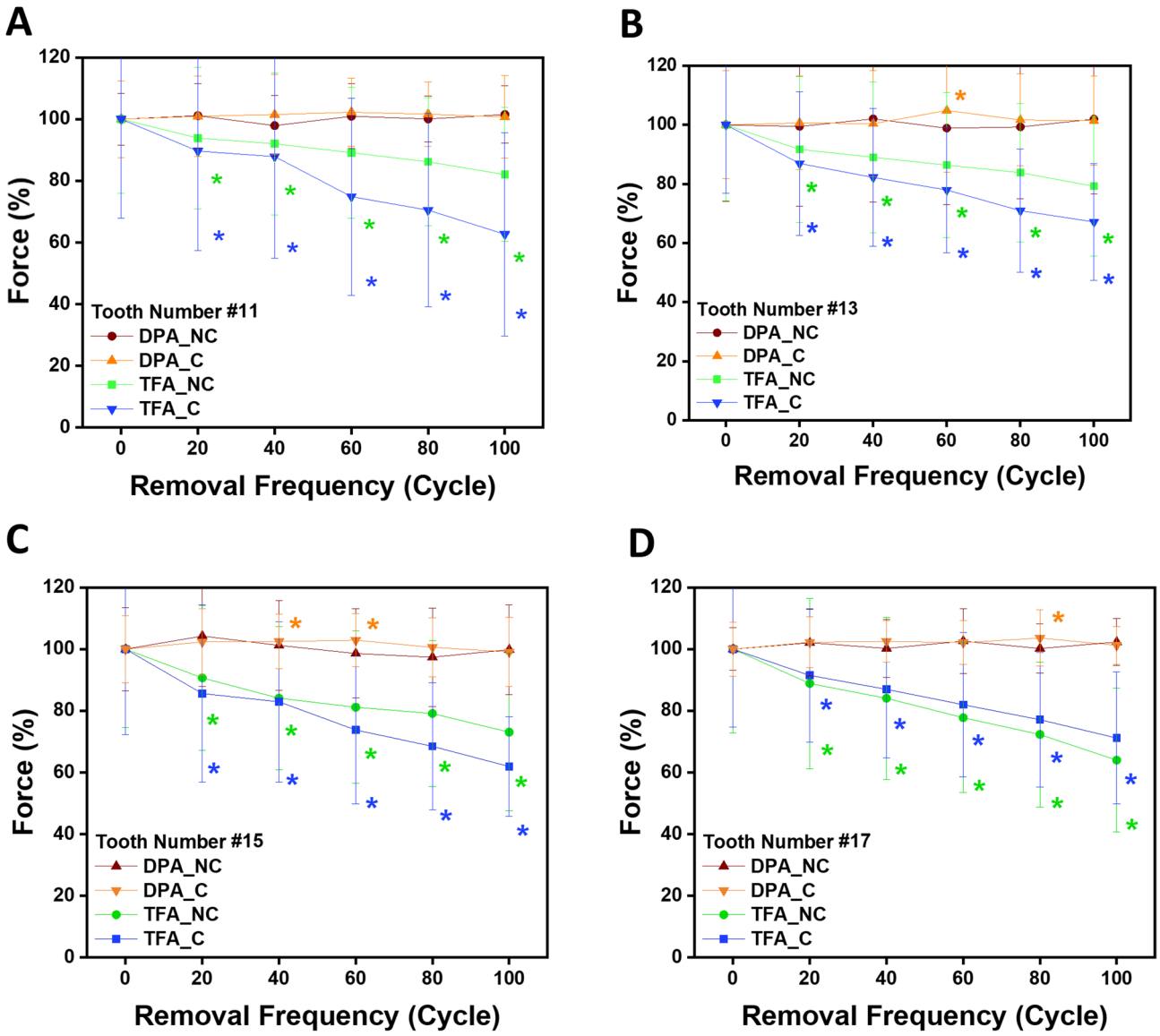

Fig. 4. Changes in force delivery of direct-printed and thermoformed clear aligners over removal frequency, expressed as a percentage. The initial force delivery is set to 100%, illustrating the relative changes in force as removal frequency increases. The panels show changes for different teeth: (**A**) Tooth #11, (**B**) Tooth #13, (**C**) Tooth #15, and (**D**) Tooth #17. Solid lines of different colors represent different groups: red for DPA_NC, orange for DPA_C, green for TFA_NC, and blue for TFA_C groups. Error bars represent standard deviation. Colored asterisks denote statistically significant changes compared to initial force (T0) for each device at each removal frequency (*$p < 0.05$), with colors matching the respective groups.

Tooth #	Surface Area	T0				T100			
		DPA_NC	TFA_NC	DPA_C	TFA_C	DPA_NC	TFA_NC	DPA_C	TFA_C
#11	PG	98.87 ± 8.43	228.01 ± 32.07	86.23 ± 16.84	298.03 ± 41.74	94.80 ± 8.39	243.59 ± 39.57	80.42 ± 14.86	303.59 ± 43.08
	P	88.93 ± 12.58	113.08 ± 27.60	92.94 ± 10.87	236.42 ± 78.52	87.26 ± 10.11	108.14 ± 26.43	86.08 ± 7.87	235.03 ± 76.73
	IN	147.11 ± 26.72	54.08 ± 8.57	141.52 ± 9.52	111.34 ± 39.25	146.59 ± 29.24	53.00 ± 9.24	131.98 ± 8.30	110.86 ± 36.88
	F	49.09 ± 3.11	4.06 ± 6.23	58.10 ± 7.85	30.61 ± 6.31	50.36 ± 2.61	3.53 ± 4.51	53.04 ± 4.15	30.60 ± 5.83
	FG	142.35 ± 37.05	97.42 ± 21.06	115.96 ± 13.65	136.34 ± 27.24	138.73 ± 36.22	104.93 ± 18.06	110.07 ± 9.22	141.21 ± 26.08
	P-value†	<0.001†††				<0.001†††			
#13	PG	89.14 ± 11.64	173.57 ± 32.36	96.39 ± 9.15	194.22 ± 121.48	87.64 ± 13.24	178.43 ± 32.60	93.70 ± 5.97	200.13 ± 123.45
	P	74.53 ± 11.81	77.63 ± 11.99	60.99 ± 11.46	93.34 ± 53.08	72.67 ± 11.24	77.15 ± 11.80	55.03 ± 13.95	93.34 ± 53.08
	IN	117.97 ± 18.34	65.88 ± 12.34	85.95 ± 19.60	151.32 ± 151.88	117.62 ± 20.31	64.62 ± 11.06	86.72 ± 16.88	146.54 ± 142.94
	F	62.73 ± 13.04	6.71 ± 4.40	99.56 ± 18.83	36.79 ± 24.02	62.78 ± 9.37	3.75 ± 2.06	98.65 ± 18.22	36.06 ± 28.65
	FG	89.09 ± 19.36	80.41 ± 13.84	135.60 ± 30.13	187.21 ± 66.32	86.98 ± 23.29	79.21 ± 10.93	135.84 ± 33.04	190.63 ± 62.62
	P-value †	0.218				0.218			
#15	PG	255.56 ± 25.49	304.54 ± 39.34	213.01 ± 59.11	316.26 ± 58.83	254.11 ± 24.03	318.20 ± 48.51	196.14 ± 47.64	324.62 ± 59.87
	P	65.88 ± 12.34	54.00 ± 8.57	79.24 ± 7.86	121.48 ± 21.05	64.52 ± 10.99	53.39 ± 7.88	80.16 ± 6.46	125.48 ± 17.37
	PC	125.57 ± 13.24	70.00 ± 9.44	118.41 ± 19.27	97.42 ± 16.84	124.34 ± 13.22	65.95 ± 6.70	110.18 ± 21.46	98.28 ± 14.42
	OF	105.12 ± 19.12	564.04 ± 50.12	112.53 ± 12.60	458.46 ± 72.94	102.57 ± 20.84	564.27 ± 49.02	112.13 ± 12.58	454.79 ± 72.49
	FC	132.17 ± 17.30	42.46 ± 6.53	149.48 ± 71.35	49.00 ± 15.94	130.41 ± 14.27	41.49 ± 6.39	124.70 ± 52.71	49.08 ± 15.38
	F	86.07 ± 13.27	33.78 ± 2.34	99.96 ± 12.40	33.47 ± 2.41	85.59 ± 12.72	32.82 ± 2.77	104.57 ± 15.39	34.22 ± 2.35
	FG	230.47 ± 38.27	99.40 ± 15.88	232.67 ± 32.58	97.19 ± 45.11	222.45 ± 29.17	99.82 ± 15.69	242.63 ± 28.22	102.93 ± 45.23
	P-value †	0.006††				0.006††			
#17	PG	123.26 ± 15.14	140.71 ± 16.97	134.00 ± 35.49	281.75 ± 79.05	122.53 ± 13.18	147.39 ± 20.16	132.90 ± 32.44	285.27 ± 76.58
	P	68.52 ± 16.81	72.15 ± 4.16	70.34 ± 10.34	77.48 ± 17.50	69.52 ± 12.91	71.01 ± 3.49	67.80 ± 8.47	80.32 ± 16.98
	PC	104.31 ± 15.31	78.93 ± 10.09	120.67 ± 26.36	68.27 ± 14.76	103.45 ± 14.74	77.05 ± 9.56	115.96 ± 26.03	66.92 ± 13.53
	OF	94.00 ± 3.66	393.70 ± 49.89	78.55 ± 9.80	268.74 ± 73.09	92.71 ± 4.63	402.28 ± 49.74	76.24 ± 11.72	267.89 ± 70.95
	FC	106.95 ± 14.36	125.51 ± 11.49	124.59 ± 17.43	98.39 ± 19.31	105.75 ± 14.07	127.27 ± 12.66	117.80 ± 17.30	101.28 ± 18.64
	F	94.68 ± 13.65	98.18 ± 7.06	60.98 ± 12.02	55.05 ± 16.81	92.16 ± 13.75	101.06 ± 8.10	62.39 ± 13.84	57.03 ± 16.41
	FG	139.93 ± 23.93	84.47 ± 14.43	143.67 ± 31.27	72.18 ± 11.39	139.08 ± 23.59	88.89 ± 14.39	141.53 ± 31.10	74.37 ± 11.08
	P-value †	0.035†				0.035†			

Table 2. Initial (T0) and after 100 removal frequencies (T100) micro-CT gap widths (μm) at each region of interest, categorized by tooth position and the presence of crowding, for two types of aligners. †Analysed linear mixed-effects model with interaction terms for surface point, appliance, and crowding presence. †, $P < 0.05$; ††, $P < 0.01$; †††, $P < 0.001$.

FG and PG areas for posterior teeth (139.93 ± 23.93 μm to 232.66 ± 32.58 μm), showing relatively uniform gap distribution.

Comparison of gap width changes between aligners: effects of crowding and tooth position

After 100 removal cycles, TFA showed significant increases in gap widths at the gingival margin areas (PG and FG) in the NC group. In contrast, the DPA_NC group exhibited significant decreases in the gap width at the FG and PG areas of the central incisors and the F area of the second molar, with no gap width changes observed at other tooth areas. In the C group, the change in gap width in the TFA_C group was reduced compared to the TFA_NC group, whereas the decrease in gap width in the DPA_C group was greater than that in the DPA_NC group. Notably, for the rearmost teeth (#17), neither aligners demonstrated significant gap width changes in the presence of crowding, except at the FC area in the DPA group. Linear mixed model analysis further revealed that, for DPA, crowding had a minimal impact on gap width changes, whereas for TFA, crowding significantly influenced the extent of gap width changes across different tooth regions, particularly for tooth #15. Interestingly, for tooth #15, the difference in the gap width changes between the PG and other regions was greater in the absence of crowding than when crowding was present in the TFA group. In the DPA group, particularly in the presence of crowding, the variance in the gap width differences between regions was large. However, owing to the small sample size and high standard deviation (SD), the statistical significance of these differences could not be determined (Fig. 5).

Discussion

This in vitro comparative study examined the impact of high removal frequency on force generation and gap width changes in DPA compared with TFA, considering different tooth positions and crowding conditions. The significance of this study lies in its potential to provide a foundational guideline for understanding how forces are applied when using DPA to effectively deliver planned forces across all teeth. Compared with TFAs, DPAs produced from each step of the digital master model consistently demonstrated more uniform fit across different

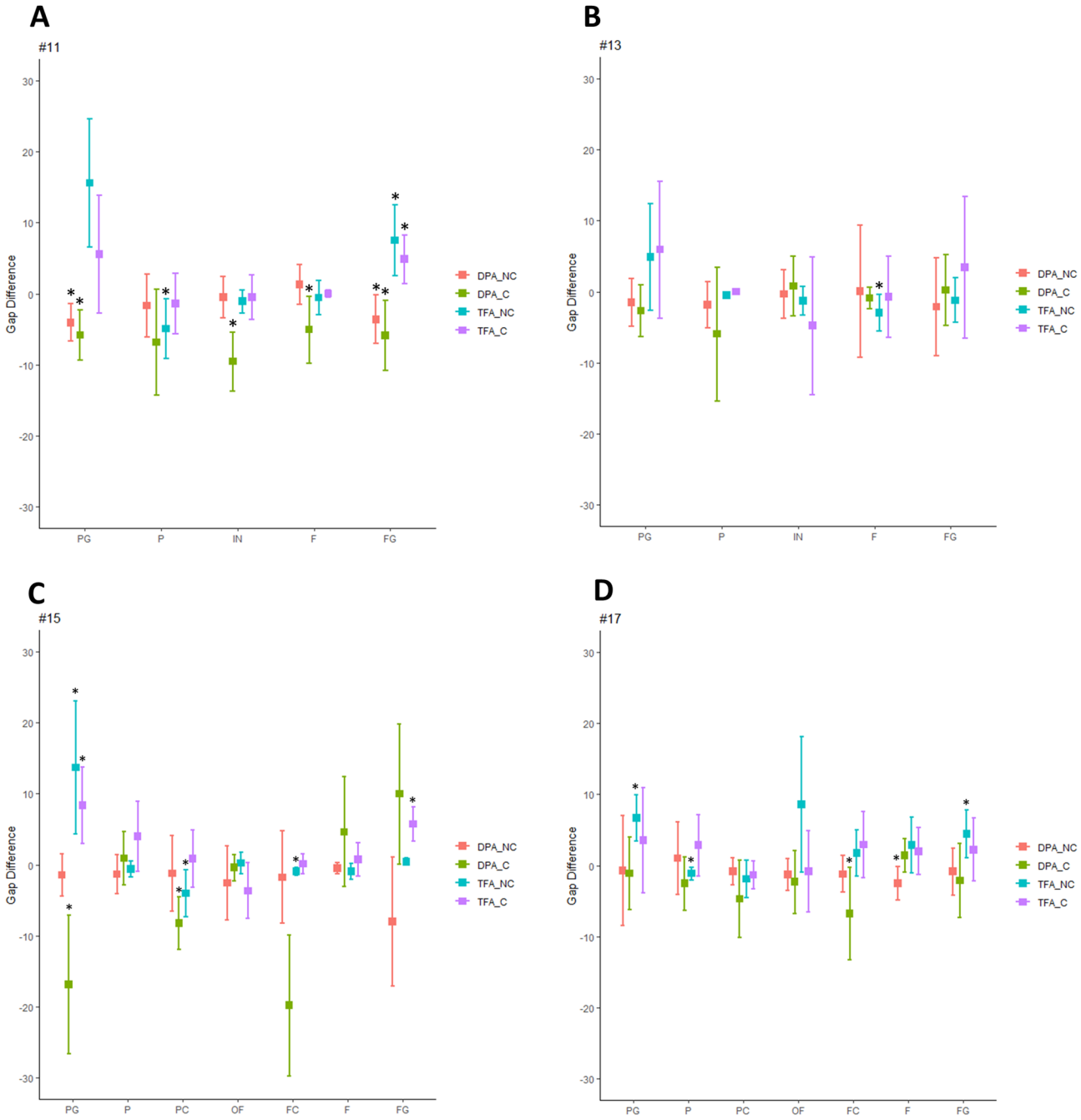

Fig. 5. The differences in gap width between the model and aligner after 100 removal cycles, comparing direct-printed and thermoformed clear aligners across various tooth regions in both crowding and non-crowding groups. The panels show changes for different teeth: (**A**) Tooth #11, (**B**) Tooth #13, (**C**) Tooth #15, and (**D**) Tooth #17.

teeth and positions from the first insertion, regardless of the degree of crowding. This lower discrepancy may ensure that the orthodontic forces are exerted relatively uniformly and as digitally planned.

This study primarily assessed the initial forces applied by each aligner to facial tooth surfaces in the same master model, correlating with site-specific aligner fit differences. Theoretically, TFA should exert no significant initial force on the master model to deliver purely programmed forces intraorally[13]. However, the initial forces from TFA were high, exceeding 100 g, when the sensor resistance and sensitivity were set to detect the minimal positive force from DPA (4–8 g). TFA exerted the greatest force on the central incisors and the least on the second molars, likely due to substantial gap discrepancies between the F and P surfaces of the incisors (Gap_F, 4.06 μm; Gap_P, 113.08 μm; Gap_PG, 228.01 μm in the TFA_NC group, and Gap_F, 30.61 μm; Gap_P, 236.42 μm; Gap_PG, 298.03 μm in the TFA_C group). This uneven aligner fit could push the incisors palatally, potentially offsetting programmed forces, and leading to unexpected or insufficient movement with TFA. In contrast, DPA

exerted low initial forces (< 7.5 g), aligning with more even gap width distribution across the tested teeth (51.09 μm to 98.87 μm in the DPA_NC group and 60.10 μm to 92.94 μm in the DPA_C group), corroborating previous findings using digital best-fit alignment algorithms[20].

Furthermore, DPA maintained lower forces steadily over increased removal frequencies, demonstrating significant dimensional stability over time, whereas the forces exerted by TFA gradually decreased, as reported in previous studies[22,24]. Lombardo et al.[25] demonstrated that thermoformed materials exhibit substantial initial stress, followed by notable stress relaxation and yield stress changes, leading to significant force loss over time. It should be noted that occasional relative force values exceeding 100% in Fig. 4 are likely due to instrumental variability and the normalization method. Such deviations can arise from measurement error, device sensitivity, or slight repositioning of the aligners during repeated removals. Despite these technical limitations, the clear difference in force stability between DPA and TFA across repeated removal cycles remains evident. Our micro-CT findings confirmed permanent TFA deformation, particularly at the gingival margins, which contributed to force loss. In the TFA_NC group, force decay was greatest in the second molars (36.28%), followed by the second premolars (27.42%), canines (21.25%), and central incisors (18.31%). In contrast, in the TFA_C group, force decay occurred in the order of the central incisors (38.95%), second premolars (36.56%), canines (33.16%), and second molars (28.41%), indicating that in cases with crowding, the reduction in force with removal frequency was more pronounced. The aligner removal frequency did not affect the force profile of DPA, which was supported by the significant dimensional stability across most of the tested surfaces.

Interestingly, the initial DPA gaps in the gingival margins were decreased by T100 in the central incisors and second premolars, improving the overall fit. The increased fit of DPA after repeated insertions and removals can be attributed to the reorganization of unstable urethane bonds. During 3D printing, urethane acrylate oligomers in DPA become fixed in a random and sterically hindered state. However, through repeated cycles of deformation and recovery, the unstable urethane bonds gradually reorganize into a more stable configuration. This process enhances the recovery force of the deformed polymer, resulting in an improved fit and better mechanical performance over time[11,14,23]. This reduction in the gingival gap width observed with DPAs after repeated removal cycles may have important clinical implications. Improved fit in the gingival margin region could enhance the precision and predictability of force delivery, leading to more effective tooth movement and potentially reducing undesired side effects such as tissue irritation or aligner instability. In contrast, TFA exhibited an increase in gingival margin gaps by T100 in the central incisors, second premolars, and second molars, indicating that changes in the gingival margin area were the most significant differences. Consequently, DPA is likely to deliver more predictable orthodontic forces as programmed, even after 100 removal cycles, with no significant differences in the overall gap and with improved fit.

A key aspect of this study was the examination of the impact of crowding on force profiles and dimensional stability. The low and constant initial loading forces of DPA remained unaffected by moderate tooth irregularity, showing no crowding-dependent gap width differences. This contrasts with TFA, where crowding led to significant initial force reductions and increased gap widths around overlapping teeth. Specifically, the P surfaces of the central incisors and canines showed increased gaps due to lingually blocked lateral incisors, reducing the undesired initial forces observed in the TFA_NC group. However, this may limit the alignment efficiency in the target movement areas, highlighting design considerations. Notably, compared to the noncrowded models, the crowded models exhibited a greater TFA force decay, especially in the central incisors, while there were no significant differences observed in the second molars. Thus, the performance of TFA may be highly susceptible to intraoral conditions, such as crowding and tooth position, leading to unpredictable outcomes. Fiori et al.[26] found clinical challenges in achieving predictable movement with TFA in crowded conditions, particularly in the facial movement of the maxillary canines and first premolars. In our study, crowding was found to significantly affect gap width variation, especially in the premolar regions, suggesting that such irregular and unpredictable changes may contribute to the inefficient movement of the premolars with TFA. However, due to the design of our study, the greater gap width changes observed near the gingival area did not perfectly align with the force changes measured at the center of the crown. Consequently, owing to the geometric accuracy and reduced site-specific differences, DPA may ensure passive-fit adaptation in crowded dentition, facilitating a more predictable alignment.

The effect of the removal frequency on the gap width variation further underscores the differences between DPA and TFA. Interestingly, DPA maintained a fairly constant gap width after repeated deformations, even in the presence of tooth crowding. This stability can be attributed to the viscoelastic properties of the material of DPA. Lee et al.[11] demonstrated that the stress relaxation and creep behavior of TC-85 showed less stress release at 80 °C compared with 37 °C while maintaining static force after 13 loading cycles. The elastic modulus and elasticity of TC-85 arise from temperature-dependent changes in the attractive forces between the polymer chains, indicating that soaking DPA in hot water can enhance its initial tooth adaptation, particularly in crowded dentitions. Furthermore, TC-85 is highly durable owing to its interconnected structure, which allows it to retain its shape after repeated exposure[27]. In contrast, TFA lacks shape memory properties because it is composed of a thermoplastic polymer[6,25]. When deformed in the permanent deformation region, thermoplastic polymers cannot return to their original shape. Additionally, although most polymer tests are conducted at 25 °C, the oral environment typically has a temperature of approximately 37 °C. This higher temperature transfers energy to the polymer molecules, causing them to easily lose their original shape. Conversely, the 3D network molecular structure of DPA allows it to maintain its original shape and mechanical properties even at elevated temperatures. This inherent stability ensures a consistent and reliable mechanical performance.

Our findings of improved fit of DPA over time suggest its clinical advantages over TFA in adapting to tooth position-aligned mismatches when delivered intraorally. Linjawi et al.[28] suggested wearing Invisalign for 15 days for the best aligner fit, in terms of minimum gap width, using scanning electron microscopy. The dimensional accuracy and stability of DPA, indicated by decreased gap widths and discrepancies, support timely programmed

tooth movement, emphasizing a force-driven mechanism beyond shape-driven behavior. However, sample heterogeneity, as indicated by large SD values, highlights the need to minimize factors that increase the gap width, including manufacturer-recommended insertion and removal techniques.

Several factors influence aligner force levels and gap width changes. The higher initial TFA forces may have resulted from the thicker (0.75 mm) PET-G sheets used in its fabrication[29,30]. However, the thickness decreased to close to 0.5 mm according to a previous study[20], reaching DPA's thickness level. Although direct thickness comparisons were not performed, DPA demonstrated consistent thickness and dimensional accuracy across sets, unlike the site-specific thickness variations in TFA[8,31]. Critically, the lowest thickness was on the facial surfaces of the central incisors, where the greatest force was exerted by the active TFA fit from vacuum compression. Thus, the dimensional accuracy with passive-fit adaptation may be more crucial than thickness differences. The vacuum thermal bonding process of TFA has limitations and requires adequate interproximal blocking to prevent patient discomfort. The shape memory properties of DPA eliminate this need, achieving a high fit even in intricate interproximal areas.

This study has some limitations. The sample size was small, particularly for micro-CT analysis, which limits the generalizability of the findings. Despite efforts to minimize these discrepancies, potential system errors may arise from force measurements using flat film sensors on curved tooth surfaces. The force range of the sensor was limited, necessitating the precise calibration of standardized measurements. As this was an in vitro study, it did not account for in vivo factors, such as saliva, occlusal forces, wearing time, and patient behavior, that could affect performance. Furthermore, only one type of TFA material (PET-G) was tested, which may not represent the behavior of all thermoformed aligners. Future studies should include various TFA materials, such as polyurethane and copolyester, to enhance generalizability. Additionally, the temperature conditions during aligner handling differed between groups, potentially affecting material properties and force measurements. Lastly, as this was an in vitro study using passive (non-activated) aligners, clinical relevance for force delivery during actual tooth movement is limited.

Conclusion

- DPAs maintain lower and stable orthodontic forces over repeated removal cycles compared to TFAs.
- DPAs show improved or consistent fit with reduced gap widths over time, regardless of dental crowding, ensuring predictable force delivery.
- TFAs exhibited significant force decay and dimensional changes, especially in the gingival margin areas, with sensitivity to crowding effects.
- The shape memory and viscoelastic properties of DPA materials contribute to their superior mechanical performance and dimensional stability.
- These findings suggest DPAs may reduce clinical unpredictability and improve treatment outcomes, though further in vivo validation is necessary.

Data availability

The datasets used and/or analyzed during the current study are available from the corresponding author on reasonable request.

Received: 20 June 2025; Accepted: 16 September 2025
Published online: 21 October 2025

References

1. Gold, B. P., Siva, S., Duraisamy, S., Idaayath, A. & Kannan, R. Properties of orthodontic clear aligner materials-a review. *J. evol. med. dent. sci.* **10**, 3288–3294 (2021).
2. Pacheco-Pereira, C., Brandelli, J. & Flores-Mir, C. Patient satisfaction and quality of life changes after invisalign treatment. *Am. J. Orthod. Dentofac. Orthop.* **153**, 834–841. https://doi.org/10.1016/j.ajodo.2017.10.023 (2018).
3. Zhang, B. et al. Effect of clear aligners on oral health-related quality of life: A systematic review. *Orthod. Craniofac. Res.* **23**, 363–370. https://doi.org/10.1111/ocr.12382 (2020).
4. Bruni, A., Serra, F. G., Gallo, V., Deregibus, A. & Castroflorio, T. The 50 most-cited articles on clear aligner treatment: A bibliometric and visualized analysis. *Am. J. Orthod. Dentofac. Orthop.* **159**, e343–e362. https://doi.org/10.1016/j.ajodo.2020.11.029 (2021).
5. Ghislanzoni, L. H. et al. How well does invisalign ClinCheck predict actual results: A prospective study. *Orthod. Craniofac. Res.* **27**, 465–473. https://doi.org/10.1111/ocr.12752 (2024).
6. Papadimitriou, A., Mousoulea, S., Gkantidis, N. & Kloukos, D. Clinical effectiveness of Invisalign(R) orthodontic treatment: a systematic review. *Prog Orthod.* **19**, 37. https://doi.org/10.1186/s40510-018-0235-z (2018).
7. Robertson, L. et al. Effectiveness of clear aligner therapy for orthodontic treatment: A systematic review. *Orthod. Craniofac. Res.* **23**, 133–142. https://doi.org/10.1111/ocr.12353 (2020).
8. Jindal, P., Juneja, M., Siena, F. L., Bajaj, D. & Breedon, P. Mechanical and geometric properties of thermoformed and 3D printed clear dental aligners. *Am. J. Orthod. Dentofac. Orthop.* **156**, 694–701. https://doi.org/10.1016/j.ajodo.2019.05.012 (2019).
9. Bruni, A., Serra, F. G., Deregibus, A. & Castroflorio, T. Shape-Memory polymers in dentistry: systematic review and patent landscape report. *Mater. (Basel).* **12** https://doi.org/10.3390/ma12142216 (2019).
10. Can, E. et al. In-house 3D-printed aligners: effect of in vivo ageing on mechanical properties. *Eur. J. Orthod.* **44**, 51–55. https://doi.org/10.1093/ejo/cjab022 (2022).
11. Lee, S. Y. et al. Thermo-mechanical properties of 3D printed photocurable shape memory resin for clear aligners. *Sci. Rep.* **12**, 6246. https://doi.org/10.1038/s41598-022-09831-4 (2022).
12. Pratsinis, H. et al. Cytotoxicity and estrogenicity of a novel 3-dimensional printed orthodontic aligner. *Am. J. Orthod. Dentofac. Orthop.* **162**, e116–e122. https://doi.org/10.1016/j.ajodo.2022.06.014 (2022).
13. Hertan, E., McCray, J., Bankhead, B. & Kim, K. B. Force profile assessment of direct-printed aligners versus thermoformed aligners and the effects of non-engaged surface patterns. *Prog Orthod.* **23**, 49. https://doi.org/10.1186/s40510-022-00443-2 (2022).
14. Schupp, W. et al. Shape memory aligners: a new dimension in aligner orthodontics. *J. Aligner Orthod.* **7**, 113–127 (2023).

15. Grant, J. et al. Forces and moments generated by 3D direct printed clear aligners of varying labial and lingual thicknesses during lingual movement of maxillary central incisor: an in vitro study. *Prog Orthod.* **24**, 23. https://doi.org/10.1186/s40510-023-00475-2 (2023).
16. McKay, A. et al. Forces and moments generated during extrusion of a maxillary central incisor with clear aligners: an in vitro study. *BMC Oral Health.* **23**, 495. https://doi.org/10.1186/s12903-023-03136-2 (2023).
17. Sharif, M. et al. Force system of 3D-printed orthodontic aligners made of shape memory polymers: an in vitro study. *Virtual Phys. Prototyp.* **19**, e2361857 (2024).
18. Manoukakis, T., Nikolaidis, A. K. & Koulaouzidou, E. A. Polymerization kinetics of 3D-printed orthodontic aligners under different UV post-curing conditions. *Prog Orthod.* **25**, 42. https://doi.org/10.1186/s40510-024-00540-4 (2024).
19. Lombardo, L. et al. MicroCT X-ray comparison of aligner gap and thickness of six brands of aligners: an in-vitro study. *Prog Orthod.* **21** https://doi.org/10.1186/s40510-020-00312-w (2020).
20. Park, S. Y. et al. Comparison of translucency, thickness, and gap width of thermoformed and 3D-printed clear aligners using micro-CT and spectrophotometer. *Sci. Rep.* **13**, 10921. https://doi.org/10.1038/s41598-023-36851-5 (2023).
21. Koenig, N. et al. Comparison of dimensional accuracy between direct-printed and thermoformed aligners. *Korean J. Orthod.* **52**, 249–257. https://doi.org/10.4041/kjod21.269 (2022).
22. Skaik, A., Wei, X. L., Abusamak, I. & Iddi, I. Effects of time and clear aligner removal frequency on the force delivered by different polyethylene terephthalate glycol-modified materials determined with thin-film pressure sensors. *Am. J. Orthod. Dentofac. Orthop.* **155**, 98–107. https://doi.org/10.1016/j.ajodo.2018.03.017 (2019).
23. Upadhyay, M. & Arqub, S. A. Biomechanics of clear aligners: hidden truths & first principles. *J. World Federation Orthodontists*. **11**, 12–21 (2022).
24. Elkholy, F., Schmidt, S., Schmidt, F., Amirkhani, M. & Lapatki, B. G. Force decay of polyethylene terephthalate glycol aligner materials during simulation of typical clinical loading/unloading scenarios. *J. Orofac. Orthop.* **84**, 189–201. https://doi.org/10.1007/s00056-021-00364-5 (2023).
25. Lombardo, L. et al. Stress relaxation properties of four orthodontic aligner materials: A 24-hour in vitro study. *Angle Orthod.* **87**, 11–18. https://doi.org/10.2319/113015-813.1 (2017).
26. Fiori, A. et al. Predictability of crowding resolution in clear aligner treatment. *Prog Orthod.* **23** https://doi.org/10.1186/s40510-022-00438-z (2022).
27. Niu, C. et al. Prospects for 3D-printing of clear aligners—a narrative review. *Front. Mater.* **11**, 1438660 (2024).
28. Linjawi, A. I. & Abushal, A. M. Adaptational changes in clear aligner fit with time. *Angle Orthod.* **92**, 220–225. https://doi.org/10.2319/042421-330.1 (2022).
29. Hahn, W. et al. Influence of thermoplastic appliance thickness on the magnitude of force delivered to a maxillary central incisor during tipping. *Am. J. Orthod. Dentofac. Orthop.* **136**, 12e11–12e17. https://doi.org/10.1016/j.ajodo.2008.12.015 (2009).
30. Bucci, R. et al. Thickness of orthodontic clear aligners after thermoforming and after 10 days of intraoral exposure: a prospective clinical study. *Prog Orthod.* **20**, 36. https://doi.org/10.1186/s40510-019-0289-6 (2019).
31. Tartaglia, G. M. et al. Direct 3D printing of clear orthodontic aligners: current state and future possibilities. *Materials (Basel).* **14** https://doi.org/10.3390/ma14071799 (2021).

Author contributions

JC and ND conducted experiments, analyzed the data, and were major contributors to writing the manuscript. KP and MJ played supportive roles in micro-CT imaging. HK and JC interpreted the results based on the material properties of the aligners. SK designed the study. All authors read and approved of the final manuscript.

Funding

This work was supported by the Korea Medical Device Development Fund grant funded by the Korea government (the Ministry of Science and ICT, the Ministry of Trade, Industry and Energy, the Ministry of Health & Welfare, the Ministry of Food and Drug Safety). (Project Number: 2710001573, RS-2023-00223150)

Declarations

Competing interests

The authors declare no competing interests.

Additional information

Supplementary Information The online version contains supplementary material available at https://doi.org/10.1038/s41598-025-20699-y.

Correspondence and requests for materials should be addressed to S.-J.K.

Reprints and permissions information is available at www.nature.com/reprints.

Publisher's note Springer Nature remains neutral with regard to jurisdictional claims in published maps and institutional affiliations.